



ELSEVIER

NDT&E International 35 (2002) 473–482

**NDT&E**  
international

[www.elsevier.com/locate/ndteint](http://www.elsevier.com/locate/ndteint)

## Field pattern characteristics of GPR antennas

S.G. Millard\*, A. Shaari<sup>1</sup>, J.H. Bungey

*Department of Civil Engineering, University of Liverpool, Liverpool L69 3GQ, UK*

Received 22 October 2001; revised 3 April 2002; accepted 21 April 2002

### Abstract

Sub-surface radar has become increasingly popular for carrying out completely non-invasive integrity tests on concrete structures. Commercial systems are available with a range of antenna frequencies that may be selected for an investigation. The choice of a particular antenna frequency is often a compromise between the physical size of the antenna and the penetration and resolution capabilities provided by the antenna. However, there is an interaction between a surface contact antenna and the substrate under investigation that will alter the field pattern being transmitted that may have significant implications for interpretation of results. An experimental programme is described in which the characteristics of commercially available 900 MHz and 1 GHz antennas are compared in air and when in contact with concrete and water surfaces, together with an emulsion used in previous studies to simulate the radar properties of concrete. Results are presented showing the influence of the material being measured upon the signal divergence. These effects are considered in terms of the practical implications for field-testing using radar. © 2002 Elsevier Science Ltd. All rights reserved.

*Keywords:* Radar; Antenna; Time domain; Concrete; Reflection; Resolution; Reinforcing bar

### 1. Introduction

Ground penetrating radar (GPR) has become increasingly popular in recent years as a non-destructive evaluation tool within the civil engineering community. It has been used for applications such as detecting voids and delamination within concrete slabs, riverbed scour around bridge piers, locating steel reinforcing bars and tendons. Before an investigation is carried out one of the choices that has to be made is the selection of a suitable antenna for the situation being studied. Popular antennas range from frequencies of 100 MHz to over 1 GHz and each antenna will have its own transmitting and receiving characteristics and capabilities. In general, the lower frequency antennas will be physically much larger and will transmit a pulse with a greater sub-surface penetration but will produce a result with poorer resolution of the sub-surface detail. A 3-year study has been carried out at Liverpool University to look more closely at two popular antennas, with nominal centre frequencies of 900 MHz and 1 GHz, used by civil engineers.

### 2. Radar theory

A type of antenna regularly used when studying the basic characteristics of an antenna is a short dipole. Both the length and the diameter of the antenna are very small relative to the wavelength  $\lambda$  of the radiated wave, so that the current used to excite the antenna is spatially uniform along its length. When Maxwell's equations are solved for this antenna, the solution gives a series of standard equations for the electric field  $\mathbf{E}$  and magnetic field  $\mathbf{H}$  for the antenna radiation [1],

From these equations it can be seen that:

- Due to its inverse, third power dependence on distance  $r$ , the electric field  $\mathbf{E}$  is the dominant field type in the region immediately around the antenna.
- A little further out away from the antenna the terms with inverse-distance squared dependence in these equations dominate and the electromagnetic radiation exists in both  $\mathbf{E}$  and  $\mathbf{H}$  fields. Within these two regions about the antenna the description of the electromagnetic radiation is very complex. These two regions constitute what commonly called as the *near-field* region of the antenna.
- At a distance far away from the antenna, only the inverse-distance terms in the equations dominate. Within this region the electric field  $\mathbf{E}$  and magnetic field  $\mathbf{H}$  are

\* Corresponding author. Fax: +44-151-794-5224.

E-mail address: [ec96@liv.ac.uk](mailto:ec96@liv.ac.uk) (S.G. Millard).

<sup>1</sup> Dr Shaari is currently at the Physics Department, Faculty of Science, Universiti Teknologi Malaysia.

### Nomenclature

$A_{pp}$	peak-to-peak amplitude
$A_{pp,max}$	maximum peak-to-peak amplitude
$\mathbf{E}$	electric field
$E_{max}$	maximum field strength
$\mathbf{H}$	magnetic field
$L_A$	characteristic antenna length
$P$	measured power
$P_{max}$	maximum power
$P_{pp}$	peak-to-peak power
$r$	radial distance
$r_0$	minimum radial distance
$R_{FF}$	distance to far-field boundary
$\lambda$	wavelength
$\eta$	intrinsic impedance
$\eta_0$	intrinsic impedance of free space = $(\mu_0/\epsilon_0)^{1/2} = 377 \Omega$
$\epsilon_0$	dielectric permittivity of free space = $8.845 \times 10^{-12} \text{ F/m}$
$\epsilon_r$	relative permittivity = $\epsilon/\epsilon_0$
$\phi_{BW}$	beam width of antenna signal
$\mu_0$	magnetic permeability of free space = $4\pi \times 10^{-7} \text{ H/m}$
$\omega$	angular frequency (rad/s) = $2\pi f$

in-phase and perpendicular to each other and the region is generally referred to as the *far-field* region of the antenna. The electromagnetic wave in this region is referred to as a transverse electromagnetic or plane wave.

The distance  $R_{FF}$  to the boundary of the far-field can be calculated with the following formula [2]:

$$R_{FF} \geq \frac{2L_A^2}{\lambda} + \lambda. \quad (1)$$

However, a value of  $R_{FF}$  of less than  $3\lambda$  is also taken as an overall minimum.

Most antenna characteristics that are relevant to GPR applications such as the wave polarisation, radiation field pattern and beam width are commonly defined in the far-field region of an antenna. However, notwithstanding the complexity of the electromagnetic radiation in the near-field region, most civil engineering applications using surface contact antennas are concerned with radar measurements in the near-field region.

#### 2.1. Beam width

Another basic feature of an electromagnetic wave is that the ratio of the amplitudes of the electric field  $\mathbf{E}$  to that of the magnetic field  $\mathbf{H}$  defines the intrinsic impedance of the dielectric medium. In the far-field region the intrinsic impedance  $\eta$  in Ohm ( $\Omega$ ) of a non-magnetic dielectric

medium is given by

$$\eta = \frac{E_\theta}{H_\phi} = \sqrt{\frac{\mu}{\epsilon}} = \eta_0 \sqrt{\frac{1}{\epsilon_r}}, \quad (2)$$

The average electrical power carried by the electromagnetic radiation from an antenna is given by the vector product of the electric field  $\mathbf{E}$  and the magnetic field  $\mathbf{H}$ . In the far-field region the fields  $\mathbf{E}$  and  $\mathbf{H}$  are related as in Eq. (2). It is sufficient therefore to measure either one of them when calculating the distributions of the field strength and the power in the radiation around the antenna. In practice measurements of these quantities are made on two orthogonal planes. One is perpendicular to the length and bisecting the dipole and is known as the *H-plane* and the other is parallel to the length and containing the dipole and is known as the *E-plane*. The theoretical relative field and power patterns of a short dipole antenna are shown in Fig. 1. The two points of about 71% of the maximum point in the field pattern or 50% of the maximum point in power pattern are commonly used to mark the *beam width* of the antenna radiation. Since in practice the difference between the maximum and minimum values is very large it is common to express the measured relative power in decibel (dB) defined as follows

$$\text{Relative power (dB)} = 10 \log_{10} \left( \frac{P}{P_{max}} \right), \quad (3a)$$

or

$$\text{Relative power (dB)} = 20 \log_{10} \left( \frac{E}{E_{max}} \right), \quad (3b)$$

Now  $\log_{10}(0.5) = -0.301$ , hence from Eq. (3a) the point

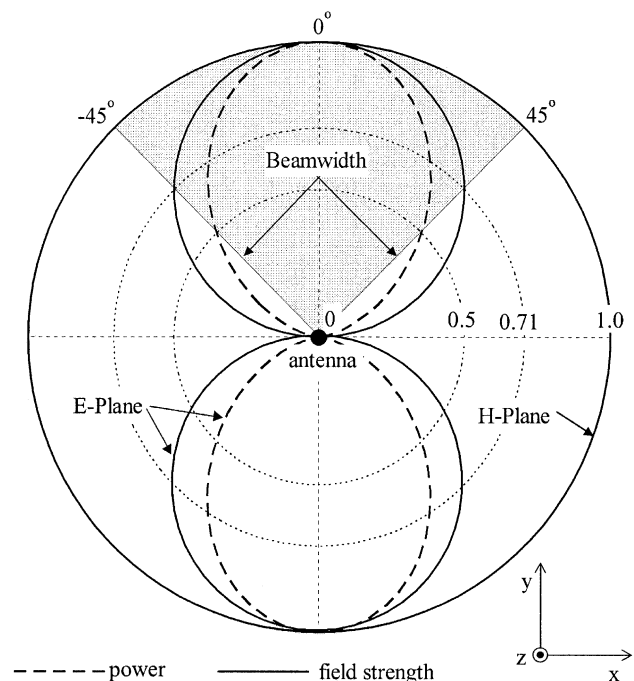


Fig. 1. Relative field and power patterns of a short dipole antenna.

where the measured power drops to a half of the maximum value is equivalent to  $-3$  dB. The beam width of the antenna can be defined then by drawing two lines from the origin through the  $-3$  dB points as shown in Fig. 1. The narrower the beam width, the higher directivity of the antenna and the better its capability to resolve closely spaced targets in the plane normal to the beam of the radiation. Due to the way the transmitting and receiving elements are arranged in a typical GPR antenna, it is the signal pattern in the  $H$ -plane that is more important for the detection and characterisation of long and thin metallic targets such as the reinforcement bars in concrete.

### 3. Characterisation of 900 MHz and 1 GHz antennas

#### 3.1. Antenna basics

The combined GPR antenna shown in Fig. 2 is made of two separate transmitter (Tx) and receiver (Rx) antennas, which are positioned at a fixed distance apart. Thus, the characteristics of an ideal short dipole antenna will be very different from those of a real GPR antenna. From the principle of reciprocity, the field pattern of an antenna when used as a transmitter must be similar to its response pattern when used as receiver [3]. It is possible to define, in a plane bisecting both the Tx and Rx antennas, a new, composite or effective field pattern for the GPR antenna, which can be considered as a superposition of the individual field patterns.

From this figure it can be seen that the effective field pattern and the effective antenna beam width  $\phi_{BW}$  will be dependent on the individual field patterns of the Tx and Rx antennas and the distance of separation between them. However, if the GPR antenna field pattern is measured directly using another GPR antenna then the measured field pattern will not be the effective pattern of the GPR antenna but that of the Tx antenna alone. The difference between the

field patterns may not be significant if the region of interest is in the far-field. However, when the target or region of interest is within the near-field then the difference could become significant. The effective field pattern in Fig. 2 only represents the antenna response in the  $H$ -plane of the GPR antenna. The effective field pattern of the combined GPR antenna in the  $E$ -plane should not be very different from that of either the individual Tx or Rx antennas regardless of the method of measurement adopted.

There is a significant difference between the geometry and means of excitation of an idealised short dipole antenna and those of a real GPR antenna. Most commercially available antennas can be divided into two types; horn (or aperture) antennas and dipole (or element) antennas. The dipole type can be subdivided further into a linear dipole or a bow-tie dipole antennas and these are shown in Fig. 3(a). Since bow-tie dipole antennas perform better as broadband radiator than horn antennas, most commercial GPR antennas, particularly those with centre frequency  $f_c$  of above 500 MHz, are bow-tie dipole antennas. The characteristic dimension,  $L_A$  for an ideal short dipole antenna is assumed to be very small compared to the wavelength  $\lambda$  of the radiated wave. This assumption, however, is not normally true for the transmitting and receiving bow-tie antennas in a commercial GPR antenna because  $L_A$  and  $\lambda$  normally are comparable in size. For a bow-tie antenna,  $L_A$  is taken as the largest antenna dimension, i.e. diagonally from one corner to the other. The effect brought about by the change of these relative sizes to the  $E$ -plane field patterns of dipole antennas in air is shown in Fig. 3(b).

This shows that the field patterns of the realistic, half-wavelength ( $\lambda/2$ ), linear and bow-tie dipole antennas are narrower than that of an idealised short dipole antenna. The field pattern shown of the short and linear dipole antennas are theoretical ones while that of the bow-tie antenna is from experimental results. As shown in Fig. 1, the field pattern of a short dipole antenna in the  $H$ -plane has no directivity due to the symmetry of the antenna geometry. Whilst a linear antenna shares the same symmetry property, this cannot be extended to the bow-tie antenna since it has a planar geometry. A theoretical study, however, indicates that as the ratio of  $L_A$  to  $\lambda$  decreases, the field pattern shows some improvement in its directivity in the  $H$ -plane of the bow-tie antenna.

Behind each Tx and Rx bow-tie antenna is a semi-cylindrical metal reflector, which enhances the emitted radiation in a forward direction [4]. This also means that the spatial dependence of the radiation from a bow-tie antenna of a GPR antenna will be different from that of a bow-tie antenna in a free space. The Tx and Rx antennas and all other components are enclosed in a metal casing, which covers the antenna on all sides except one, which functions as the antenna aperture. This metal casing acts as an electromagnetic shielding for GPR users and thus helps prevent antenna proximity effects with the operator from downgrading the overall performance of the antenna.

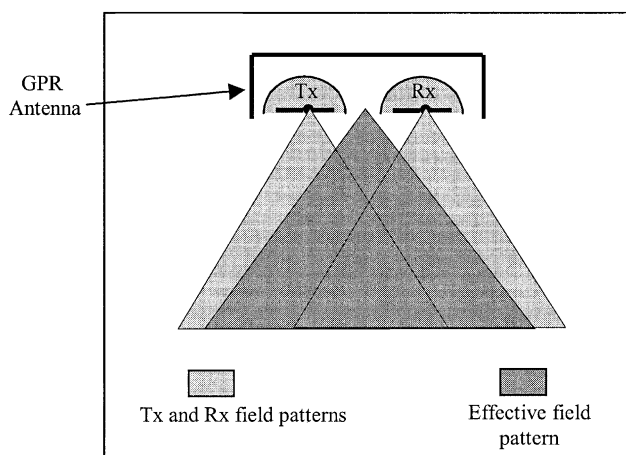


Fig. 2. Model for the effective field pattern of a GPR antenna. (a) Linear and bow-tie dipole antennas and (b) field patterns in the far-field.

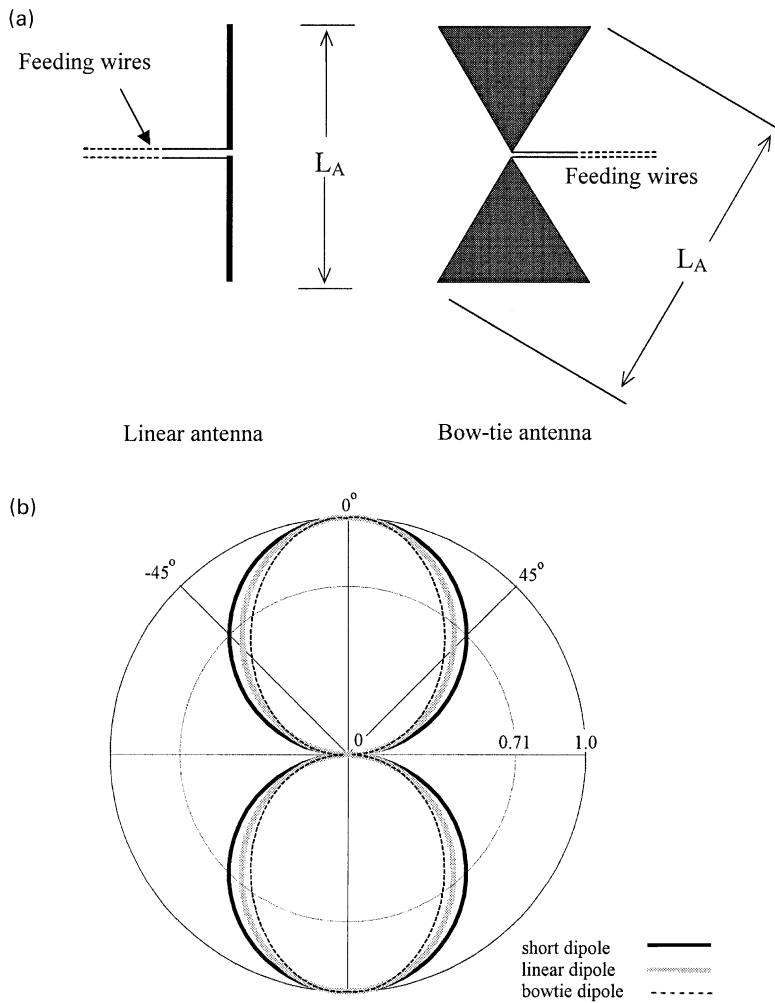


Fig. 3. Geometry and field patterns of dipole antennas.

3.2. Coupling effects of antenna on a dielectric interface

In order to maximise the transmitted radiation, a dipole type GPR antenna is coupled directly onto the dielectric medium surface. It is necessary to understand how the effective field pattern of the antenna, and thus its effective beam width  $\phi_{BW}$ , will be different from those when the antenna is in free space. Equally important is the knowledge of the effects on the centre frequency  $f_c$ , the bandwidth  $\Delta f$  and the spatial dependence of the GPR antenna radiation in the dielectric medium. These effects have been published elsewhere [5].

There have been a number of theoretical studies on the effects of the antenna–medium coupling on antenna characteristics. Most of these were focused on a short dipole antenna placed near or on the surface of a semi-infinite, homogeneous medium [6]. Fig. 4 shows some typical results of the effects of the medium permittivity  $\epsilon'_r$  upon the field patterns of the antenna in the  $H$ -plane.

It can be seen that higher the permittivity  $\epsilon_r$ , the more electromagnetic radiation is transmitted into the dielectric

medium. In addition, there is a significant difference between the field patterns of the short dipole antenna in air compared to when it is on a dielectric interface. These field patterns only represent the antenna characteristics in the far-field region and have been experimentally verified using a planar dipole antenna.

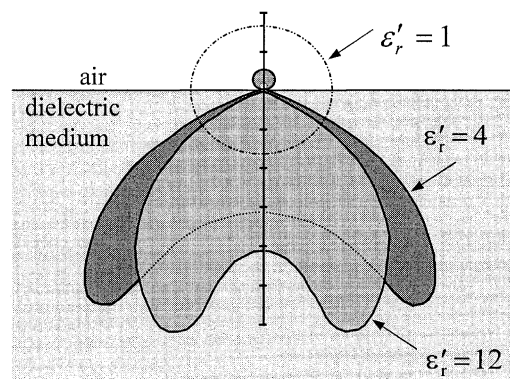


Fig. 4. Field pattern in the  $H$ -plane of a short dipole antenna on a dielectric interface.



### 3.3. Measurement methods for GPR antennas

#### 3.3.1. Principles of field pattern measurement

In order to determine the beam width  $\phi_{BW}$  of an antenna, the field pattern is measured on one of the  $E$  and  $H$  planes of the antenna. Both the beam width  $\phi_{BW}$  and the field pattern are used to describe the characteristics of the antenna in its far-field region, calculated using Eq. (1). However, the field pattern measurement for an antenna can be carried out either in the near-field region or the far-field region and it can be done directly or indirectly.

#### 3.3.2. Direct measurement

For direct measurement a field probe comprising a small and well characterised antenna is used to measure a certain component of the electric field  $\mathbf{E}$  in the radiation emitted by the antenna under test at a series of measurement points along a line formed by the intersection between the  $E$  or  $H$  plane of the antenna and the measurement surface. The measurement surface can be a plane, a spherical surface, or a cylindrical surface and can be located either in the near-field or the far-field region of the antenna. However, when the antenna measurement is carried out in the near-field region its field pattern in the far-field region is normally determined by performing a near-to-far-field transformation of the near-field data [2]. For this study, measurement is carried out by scanning a second GPR antenna along a plane that is perpendicular to the main beam of the GPR antenna under study, Fig. 5(a). A measurement is taken of the field strength at discrete points along two lines; one lies in the  $E$ -plane while the other in the  $H$ -plane of the antenna.

#### 3.3.3. Indirect measurement

An alternative method of characterising a GPR antenna is by measuring the reflected signal from a simple target with well known scattering properties using the same GPR antenna for transmission and receiving, Fig. 5(b). Due to their high symmetry and high reflectivity two common targets used in this type of measurement are those of the metal sphere and metal bars. This approach is considered as an indirect method since the actual field strength at any measurement point in the antenna radiation is never directly measured. When using the direct method for measuring the field pattern of an antenna on a surface dielectric medium there is always a problem associated with limited access and the freedom to move the field probe in the dielectric medium, which could be in the form of a solid or liquid. In this situation indirect methods may provide a number of advantages over the direct method.

One of the main advantages of the indirect method of measurement over that of the direct method is that it can be expected to provide a better description of the field pattern of a combined GPR antenna because it incorporates the field patterns of both the transmitting Tx and receiving Rx

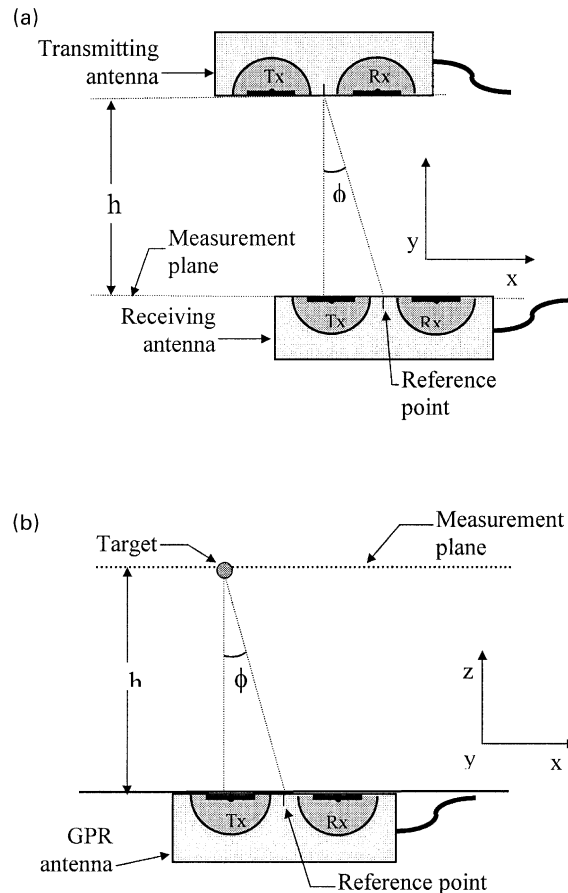


Fig. 5. Measurement planes and reference points in antenna measurements.

antennas of the GPR antenna and thus the measurement is a better representation of the effective field pattern of the antenna, as shown in Fig. 3.

A comparison of the direct and indirect methods in an earlier paper [5] has shown that both methods give very similar results for measurements of the radar signal. In practice, depending on the size and geometry of the target used and the various approximations adopted, there are several indirect methods that can be used to measure an antenna field pattern. Two methods which have been used in this study are the *radar equation* [7] and the *wire scattering* [8] methods.

### 3.4. Geometries of the 900 MHz and 1 GHz antennas

The two GPR antennas studied are the 900 MHz antenna (Model 3101D) and the 1 GHz antenna (Model 3100) manufactured by Geophysical Survey Systems, Inc. [9]. Typical geometries of these antennas and details of their physical dimensions are shown in Fig. 6. The 900 MHz antenna incorporates some of its initial-stage transmitting and receiving circuits within the antenna casing while the 1 GHz antenna houses the corresponding electronic in a separate box, connected by an additional cable.

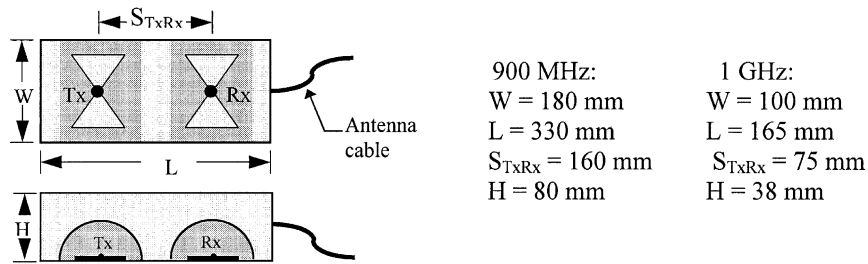


Fig. 6. Geometries and dimensions of 900 MHz and 1 GHz antennas.

### 3.5. Far-field boundaries of the GPR antennas

Depending on the types of antenna, the field pattern in the near-field region can be quite different from that in the far-field region. The field pattern of an antenna measured in its near-field region normally depends on the distance from the antenna [10]. Before the field pattern of a GPR antenna is measured it is necessary to determine whether the measurement is being made is in the antenna near-field region or not using Eq. (1). Measurements of the actual centre frequencies of the nominal 900 MHz and 1 GHz antennas show [5] somewhat lower values of 836 and 887 MHz, respectively. These measurements give a centre wavelength,  $\lambda_c$  in air of 359 and 338 mm, respectively. Using the antenna dimensions shown in Fig. 6, the characteristic or maximum dimension  $L_A$  of the 900 MHz and 1 GHz antenna are 230 and 120 mm, respectively, where  $L_A$  is taken as the diagonal length of the transmitting antenna, Fig. 3(a). This gives a far-field boundary  $R_{FF}$  for the 900 MHz antenna in air of 654 mm, while that of the 1 GHz antenna is 423 mm. However, these values are only approximate and notwithstanding these results, values of  $3\lambda_c$  are also often used, giving far-field boundaries of 1077 and 1014 mm for the two antennas.  $R_{FF}$  will be different in other materials such as concrete, where the wavelengths will be longer. Measurements in concrete [5] have shown centre frequencies of the nominal 900 MHz and 1 GHz antennas to drop to 500 and 666 MHz, respectively. Thus, in concrete these measurements result in an evaluation of the far-field boundary (Eq. (1)) of 776 and 514 mm, respectively, whilst the more conservative  $3\lambda_c$  values are 1077 and 1014 mm, respectively.

## 4. Measurement of antenna field patterns in air

### 4.1. Direct (bistatic) and indirect (monostatic) measurements

The antenna or the target is held fixed in the air by a wooden structure. For monostatic measurements the antenna is held fixed in the middle of a trolley that is free to move along tracks. For bistatic measurements the antenna is hung from another wooden support while a receiving antenna is mounted on the trolley. The height of the target

can be up to 1500 mm from the antenna for monostatic measurements while for bistatic measurements the antenna can be up to 1200 mm from the receiving antenna, placing the targets into the far-field. For bistatic measurements the  $H$ -plane measurement is taken with both the transmitting and the receiving antennas parallel to the direction of scanning, Fig. 5(a). For monostatic measurements using a long metal bar for a target, the  $H$ -plane measurement is taken with both the scanning direction and the length of the antenna perpendicular to the bar, Fig. 5(b).

An antenna field pattern describes the angular distribution of either the relative field strength or the power in the electromagnetic radiation. If  $A_{pp,max}$  is the maximum peak-to-peak amplitude of the GPR signals measured on a particular measurement plane then using Eq. (3b) the corresponding relative peak-to-peak power ( $P_{pp}$ ) in decibel (dB) can be written as follows

$$P_{pp} = 20 \log \left( \frac{A_{pp}}{A_{pp,max}} \right). \quad (4)$$

The results for both the monostatic and bistatic methods are presented in the form of the distribution of the relative power as a function of the antenna position in the  $x$ -direction. The plot of the relative power in decibel (dB) and the antenna spatial position on the measurement plane is the antenna response for the bistatic method and the echo response for the monostatic method.

### 4.2. Antenna field patterns

It can be seen from Fig. 7(a) that for the 900 MHz antenna both the widths and the shapes of the responses from the two measurement methods are very similar. At the  $-3$  dB level the width of the antenna response using the bistatic method is 460 mm while that of the echo response using the monostatic method is 450 mm. For the 1 GHz antenna it can be seen from Fig. 7(b) that the width of the antenna response (590 mm) is slightly larger than that of the echo response (540 mm). These results indicate that the monostatic method can be used effectively to estimate the effective  $H$ -plane field pattern of a GPR antenna. It can also be seen from Fig. 7(a), there is little difference between the echo response using a target bar with 20 and with 10 mm diameter.

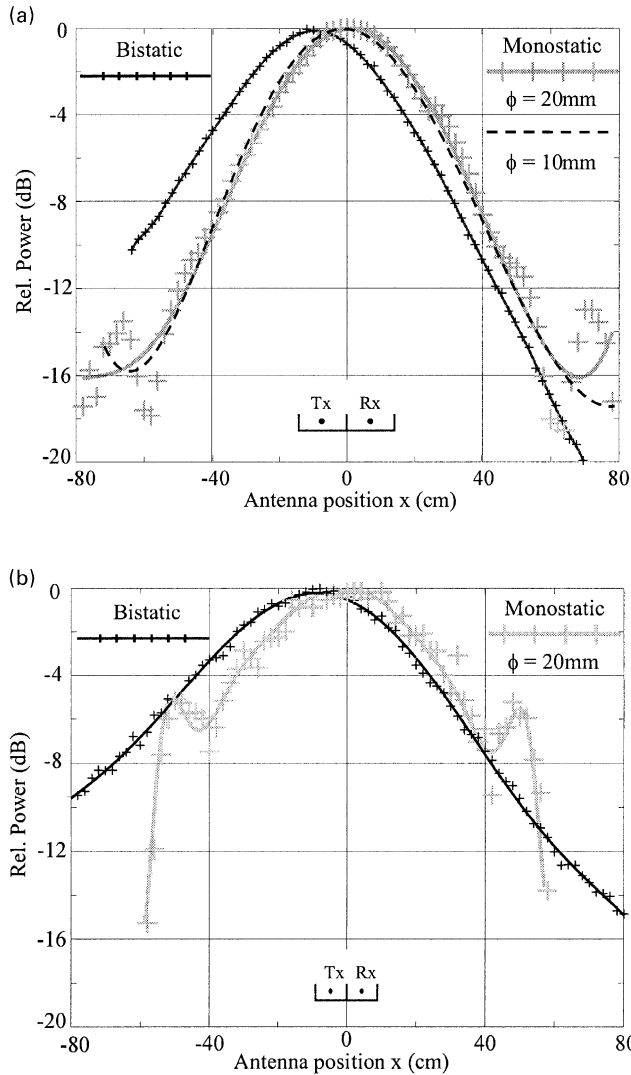


Fig. 7. Responses of GPR antennas in air.

### 4.3. Spatial attenuation

The spatial attenuation of a GPR antenna can be assumed to vary according to an inverse-distance (radius) dependence and it can be shown that the amplitude loss due to the spatial attenuation can be calculated from the ratio of the radial distance  $r$  of each of the measurement points to a minimum radial distance  $r_0$ . This is the separation distance between the measurement plane and a parallel plane that passes through the target for monostatic measurements or the aperture of the receiving antenna for bistatic measurements. The spatial loss (SL) in decibel (dB) can be calculated using an equation similar to Eq. (4):

$$\text{Spatial loss (SL)} = 20 \log\left(\frac{r}{r_0}\right). \quad (5)$$

Fig. 8(a) shows both monostatic and bistatic spatial attenuation of the 900 MHz antenna in air. The curves representing the inverse-distance and the inverse-distance square dependence are also shown. These results show that

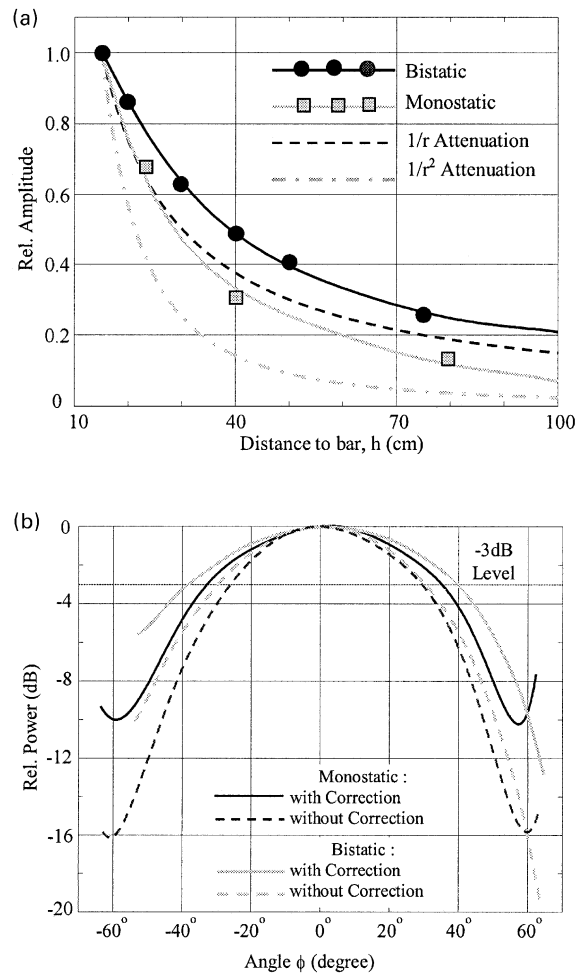


Fig. 8. Spatial attenuation and field patterns for 900 MHz antenna in air. (a) Typical echo responses of antenna and (b)  $H$ -plane field pattern of antenna.

the spatial attenuation for monostatic measurements lies much closer to the inverse-distance dependence than that of the bistatic method. Spatial attenuation for a bistatic measurement represents one-way attenuation of the radar signal whilst a monostatic measurement represents two-way attenuation. Ideally an inverse-distance dependence can only be achieved when the radiation is emitted by a point source. For a real antenna this can be achieved only in the far-field region. The fact that the bistatic spatial attenuation is higher than the inverse-distance dependence is consistent with the type and design of the GPR antenna. The metal reflector behind the transmitting (Tx) bow-tie antenna reinforces some of the radiated energy in the forward direction. For comparison purposes the inverse-distance dependence for spatial attenuation of the 900 MHz GPR antenna is adopted.

From Fig. 6 the angular position  $\phi$  of each of the measurement points on the measurement plane can now be calculated using:

$$\phi = \arctan\left(\frac{x}{h}\right). \quad (6)$$

Table 1  
3 dB beam width  $\phi_{\text{BW}}$  in the  $H$ -plane for 900 MHz and 1 GHz antennas in air

GPR antenna	900 MHz			1 GHz	
	Bistatic	Monostatic ( $\phi = 20$ mm)	Monostatic ( $\phi = 10$ mm)	Bistatic	Monostatic ( $\phi = 20$ mm)
Uncorrected 3 dB beam width $\phi_{\text{BW}}$	60°	56°	56°	73°	62°
Corrected 3 dB beam width $\phi_{\text{BW}}$	77°	69°	68°	105°	73°

Thus the uncorrected  $H$ -plane field pattern of the antennas is obtained by plotting the relative peak-to-peak power ( $P_{\text{pp}}$ ) in decibel (dB) calculated using Eq. (4) against the angle  $\phi$  in degrees. Similarly the corrected field pattern of an antenna is represented by a plot of the sum of the peak-to-peak power ( $P_{\text{pp}}$ ) and the spatial loss (SL) versus the angle  $\phi$ .

The bistatic and monostatic,  $H$ -plane field patterns for both the 900 MHz and 1 GHz antennas in air are shown in Fig. 8(b). The beam width  $\phi_{\text{BW}}$  of these antennas can be determined from the width at the  $-3$  dB level of the corresponding field patterns. The results are summarised in Table 1.

- From the results in air it can be seen that:
- Both the monostatic and bistatic  $-3$  dB beam widths  $\phi_{\text{BW}}$  for the 1 GHz antenna are larger than those of the 900 MHz antenna.
- The beam width  $\phi_{\text{BW}}$  measured using the monostatic method is smaller than when using the bistatic method. For the uncorrected beam widths  $\phi_{\text{BW}}$  the difference is about 4° (7%) for the 900 MHz and about 11° (18%) for the 1 GHz antenna.
- The beam width  $\phi_{\text{BW}}$  corrected for spatial attenuation (which is assumed to vary with an inverse-distance dependence) increases by 13–32°.
- For the monostatic results of the 900 MHz antenna there is a very little difference in the beam widths  $\phi_{\text{BW}}$  measured using targets with different diameters.

The corrected bistatic beam widths  $\phi_{\text{BW}}$  of 77° for the 900 MHz antenna is quite close to the beam width  $\phi_{\text{BW}}$  of 79° reported by BAM [11].

## 5. Measurement of sub-surface antenna field patterns

The principal objective of this study is to use the monostatic method to measure the characteristics of a GRP antenna on a concrete surface. It has been demonstrated that the  $H$ -plane field pattern from a monostatic measurement can be considered as the effective field pattern of a GPR antenna while that of the bistatic method represents the characteristic of the transmitting (Tx) bow-tie in the GPR antenna. In this section the monostatic method will be used to measure the  $H$ -plane field patterns of the 900 MHz and 1 GHz antennas on the surface of concrete.

The field pattern of a GPR antenna on the surface of

concrete can be significantly affected by the following factors.

- Due to the so-called coupling or proximity effect, the electrical impedance of an antenna on the surface of a dielectric medium can be different from that when the antenna is in the air. The change in the impedance has been reported as the main cause for the drop in the centre frequency  $f_c$  of the antenna.
- It has also been reported that for an antenna on a surface of a dielectric medium the field pattern in the medium can be very different from the one in air. In addition, since a dielectric medium such as concrete is a lossy medium there will always be a degree of attenuation of a GPR signal due to the material loss in addition to that caused by spatial attenuation.

### 5.1. GPR antenna on concrete surface

The characteristics of both the 900 MHz and 1 GHz antennas on a concrete surface have been studied by measuring the reflected signal from steel bar embedded in a  $700 \times 1200 \times 400$  mm<sup>3</sup> concrete (45 N/mm<sup>2</sup>) slab. All four edges of the slab were painted with bitumen paint to minimise variations in the moisture content across the width of the slab. Two steel bars with a diameter of 16 mm and length 750 mm were located at cover depths of 50 and 150 mm. The relative permittivity of the concrete was measured as 7.5.

### 5.2. GPR antenna field patterns in dielectric media

The echo responses of the 900 MHz antenna on concrete and in air are shown in Fig. 9(a). All these results are  $H$ -plane measurements with a target depth of 150 mm. For clarity only the data points corresponding to the echo response of the antenna on concrete surface are shown in the figure. It can be seen that there is a significant reduction in the width of the echo response of the 900 MHz antenna coupled to concrete surface compared to when it is in air.

The uncorrected  $H$ -plane field patterns of the 900 MHz antenna, as described in Section 4.3, can be obtained by plotting the echo responses in Fig. 9(a) against the angular position  $\phi$  of the measurement points. The corrected field patterns are those in which the effect of the inverse-distance attenuation upon the signal relative power is included. Effects of material attenuation have not been included.



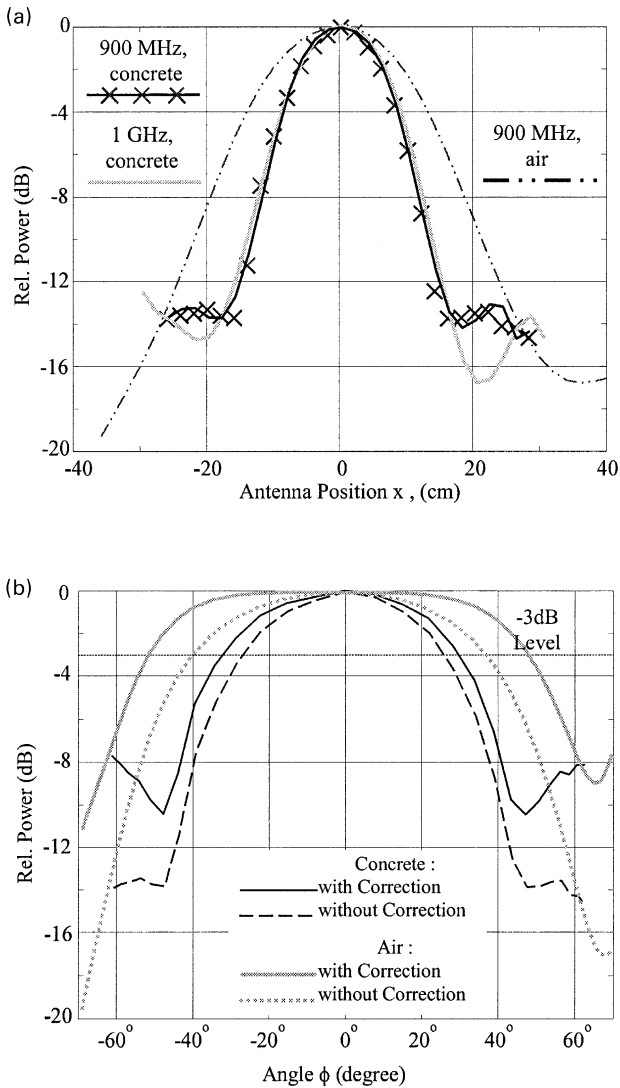


Fig. 9. Responses and field pattern of 900 MHz antenna in air and on concrete surface.

However, for dry concrete with a low conductivity these are expected to be quite small. Both the corrected and the uncorrected effective field patterns of the 900 MHz antenna in air and on the concrete surface are shown in Fig. 9(b). The effective  $-3$  dB beam width  $\phi_{BW}$  of the 900 MHz antenna and those of 1 GHz antenna are shown in Tables 2 and 3, respectively.

From the results it can be seen that there is a significant decrease in the effective beam widths  $\phi_{BW}$  of both the 900 MHz and 1 GHz antenna on the concrete surface compared to their beam widths  $\phi_{BW}$  in air. The results indicate that the effective beam width of a GPR antenna on the surface of a dielectric medium decreases as the relative permittivity increases.

### 6. Discussion

The significance of these studies of antenna beam width

Table 2

3 dB beam width of 900 MHz antenna on surface of concrete

Medium	Bar diameter (mm)	Uncorrected 3 dB beam width $\phi_{BW}$	Corrected 3 dB beam width $\phi_{BW}$
Air	20	77°	100°
Concrete	16	53°	62°

Table 3

3 dB beam width of 1 GHz antenna on surface of concrete

Medium	Bar diameter (mm)	Uncorrected 3 dB beam width $\phi_{BW}$	Corrected 3 dB beam width $\phi_{BW}$
Air	20	104°	N/A
Concrete	16	55°	64°

is in the resolution that would be expected from an antenna in distinguishing between closely spaced targets. It is expected that a higher frequency antenna with a shorter wavelength signal will be more effective in separating two adjacent targets into discrete signal reflections. However, a higher frequency antenna normally has a poorer signal penetration into a lossy medium. Thus, low frequency antennas are chosen to detect targets deep beneath the surface, particularly if the medium has a high conductivity (high loss), but it is accepted that the detection of small targets or the separation of the two targets with a close lateral spacing will be poorer than would be expected if a higher frequency antenna was selected. On the other hand, a high frequency antenna would not be expected to transmit a signal as far through a lossy medium.

When comparing the two antennas in air, it is somewhat surprising that the lower frequency 900 MHz antenna has a narrower measured beam width than the 1 GHz antenna and thus would be expected to have a better resolution capability. However, once both antenna are placed upon a relatively dry concrete surface both the beam width were measured to be very similar and thus their resolution capabilities would be expected to be similar too. However, the 900 MHz antenna would still be expected to have an improved penetration capability and is normally the antenna of choice.

### 7. Conclusions

In this paper the characteristic field patterns and signal waveforms of the 900 MHz and 1 GHz GPR antennas, both in air and on a concrete surface have been studied with two different methods: the direct/bistatic method and the indirect/monostatic method.

#### 7.1. Characteristics of GPR antennas in air

- (i) The field pattern and beam width  $\phi_{BW}$  from the monostatic and bistatic measurements represent two

different aspects of the effective characteristics of a GPR antenna. In the monostatic method the measured field pattern and  $-3$  dB beam width  $\phi_{\text{BW}}$  represent the corresponding effective characteristics of the combined GPR antenna. In the bistatic method the results represent the characteristics of the transmitting (Tx) bow-tie antenna within the combined GPR antenna.

- (ii) The monostatic method is a preferred and more practical method to the bistatic method because it uses only a single combined Tx/Rx antenna and does not rely upon a second antenna located within the dielectric medium being studied.
- (iii) At a distance 400 mm from the antenna the uncorrected beam width  $\phi_{\text{BW}}$  from the two methods differ by 4% for the 900 MHz antenna and 18% for the 1 GHz antenna.
- (iv) In its near-field region the spatial attenuation of the 900 MHz antenna does not exactly follow an inverse-distance dependence. Thus, the results obtained from adding the contribution from the spatial loss with an assumed, inverse-distance dependence to the uncorrected field pattern and beam width  $\phi_{\text{BW}}$  can be misleading.
- (v) In the monostatic method where the target is a long steel bar the results in the uncorrected field pattern and beam width  $\phi_{\text{BW}}$  are not significantly affected by changes in the bar diameter.

### 7.2. Characteristics of GPR antenna on concrete surface

- (i) At a target depth of 150 mm it is found that the uncorrected, effective 3 dB beam width  $\phi_{\text{BW}}$  of the 900 MHz and 1 GHz antennas on a concrete surface drop to about 69 and 53% of respective values in air.

- (ii) For an antenna on a concrete surface, it is found that there is little difference between the effective beam width  $\phi_{\text{BW}}$  of the 900 MHz and 1 GHz antennas. The difference between the two beam widths  $\phi_{\text{BW}}$  is less than 4% which means as far as the horizontal resolution  $\Delta_{\text{H}}$  of a GPR antenna is concerned there is no significant advantage of using either one of the two GPR antennas.

### References

- [1] Liao SY. Engineering applications of electromagnetic theory. New York: West Publishing Company; 1988. Chapter 9.
- [2] Yaghjian AD. Review of near-field antenna measurements. *IEEE Trans Antenna Propag* 1986;34(1):30–45.
- [3] Stutzman WL, Thiele GA. Antenna theory and design. New York: Wiley; 1981. p. 260–1.
- [4] Macnamara T. Handbook of antennas for EMC. Artech House; 1995. Chapter 5; p. 140.
- [5] Millard SG, Shaari A, Bungey JH. Frequency characteristics of GPR antennas. *Insight* 2001;43(7):450–7.
- [6] Smith GS, Scott Jr. WR. Scale model for studying ground penetrating radar. *IEEE Trans Geosci Remote Sensing* 1989;27(4):358–63.
- [7] King RWP, Blejer DJ, Sandler BH. Current induced on single and crossed electrically short and thin tubular cylinders by a normally incident plane electromagnetic wave. *IEEE Trans Antenna Propag* 1979;27(5):624–33.
- [8] Calazans ET, Griffiths HD, Cullen AL, Benjamin R, Davies DEN. Antenna pattern measurement using a near field wire scattering technique. *Int Conf Antenna Propag (ICAP 89)* 1989;341–4.
- [9] GSSI. Antenna electrical specifications. USA: Geophysical Survey Systems; 1992.
- [10] IEEE. IEEE standard test procedures for antennas. The Institute of Electrical and Electronics Engineers; 1979. p. 139.
- [11] BAM. Determination of the dielectric properties of brick and mortar. Report on task 1.2 of the Brite-EuRam III subsurface radar as a tool for non-destructive testing and assessment in the construction and building industries. Berlin (Germany): Federal Institute for Materials Research and Testing (BAM); 1997. p. 5 (private communication).